

# CONCENTRATION AND SCAN RATE DEPENDENT ELECTROCHEMICAL MEASUREMENTS USING A FLOATING ELECTRODE

**Bachelor assignment report**

Wouter Kühlkamp and Bram Leemeijer

FACULTY TNW  
NANOIONICS (NI)

Tutor: Sahana Sarkar, MSc.  
Teacher: Prof. Dr. Serge Lemay  
Coordinator: Dr. Stefan Kooij

## Summary

Nanogap devices have a narrow channel of 65 nm height with electrodes on both sides. These devices have such small volumes that they can be used to detect single molecules using electrical signals. One possible new way of doing this, could be to leave one electrode floating while sweeping the other electrode and looking at the charge that is built up on the floating electrode.

In this report the influence of the concentration of 1,1-ferrocenedimethanol that is inside a nanogap device and the scan rate on the charge that is built up on the floating electrode is researched. Furthermore the influence of measuring equipment and the lifespan of the nanofluidic device are investigated.

The expectation for the concentration dependency is that a lower concentration of molecules would cause the floating electrode to follow the applied potential less, since there are fewer molecules that can transfer charge. For the scan rate dependency the expectation is that a slower scan rate would cause the floating electrode to follow the applied potential better, since a slower scan rate means that the floating electrode has more time to catch up with the electrode that is being swept.

The experimental results are that for the concentration dependency the expectation is correct for concentrations of 1  $\mu\text{M}$  1,1-ferrocenedimethanol and higher, but for concentration lower than 1  $\mu\text{M}$  it doesn't work, concluding that the limit of this technique at room temperature is somewhere between 100 nM and 1  $\mu\text{M}$ . A simulation is done and confirms that the limit lies around the mentioned point. Looking at the scan rate the expectation is correct, with lower scan rates more charge builds up on the floating electrode for the same concentration. The measurement equipment employed influences the results significantly. Combined with the short lifespan of the devices, this renders the results not fully reproducible.

# Contents

<b>1</b>	<b>Introduction</b>	<b>3</b>
<b>2</b>	<b>Theory</b>	<b>4</b>
2.1	A brief introduction to electrochemistry . . . . .	4
2.2	Why nanogap devices . . . . .	4
2.3	Why is there a need for a new method? . . . . .	4
2.4	Expectations . . . . .	5
<b>3</b>	<b>Experimental Setup</b>	<b>7</b>
3.1	Device fabrication and geometry . . . . .	7
3.2	Measurement preparation and setup . . . . .	10
<b>4</b>	<b>Results and Discussion</b>	<b>12</b>
4.1	Results . . . . .	12
4.1.1	Concentration dependent measurements . . . . .	12
4.1.2	Concentration dependent simulation . . . . .	13
4.1.3	Scan rate dependent measurements . . . . .	15
4.2	Possible problems with potential measurements in nanochannels . . . . .	16
4.2.1	Instruments used in the measurements . . . . .	16
4.2.2	Reusability of the devices . . . . .	16
4.3	Possible improvements for further research . . . . .	17
<b>5</b>	<b>Conclusion</b>	<b>18</b>
<b>6</b>	<b>Appendix</b>	<b>19</b>

# 1 Introduction

The detection of single molecules is a very challenging problem with a wide range of possible applications. Probably the most obvious and immediate one is the sequencing of DNA. Techniques based on mechanics and optics are already developed or being developed,<sup>1</sup> where electrical techniques lag behind. Yet, these techniques based on electrical detection have advantages over the previously mentioned ones; Unlike mechanical methods, electrochemical and optical methods can be incorporated with microelectronics and fluidic devices and can therefore be used in systems like Lab-on-a-Chip. The big advantage of electrochemical methods over optical ones is that the former one can be combined, cheaply, with all the necessary electronics to analyze the samples immediately.

The charges involved in a typical electrochemical process, where only a few molecules are present, are small; only a few electrons are transferred, which makes direct detection hard or even impossible. However, due to redox cycling, where molecules get repeatedly reduced and oxidized as they diffuse into the channel and shuttle between the two electrodes, the current gets amplified. These electrodes are incorporated in nanofluidic devices and, to get large enough amplification, the electrodes are spaced 65 nm from each other.<sup>2,3</sup> With single molecule detection typical currents are in the range of a few femtoamperes.<sup>4</sup> This is a problem if it has to be used in a device like Lab-on-a-Chip, because the signal-to-noise ratio is very small when detecting such a small current.

Instead of looking at currents, looking at the charge that is built up could be a possible alternative. If one electrode is left floating, while applying the cyclic potential to the other electrode, the charge build-up on the floating electrode can be measured. For low concentrations, voltages in the order of magnitude of a hundred micro volts are expected, which is less subject to noise compared to femtoampere measurements.<sup>5</sup>

The focus of this report is on precisely this type of electrostatic potential measurements. There are two questions that are going to be answered: How does the potential of the floating electrode follow the applied potential, for different concentrations and what is the lowest concentration that can be measured? And how does the scan rate influence the following of the floating electrode? The hypothesized answers to these questions will be discussed in section 2 Theory.

The theoretical and experimental aspects are first discussed in this report, followed by a discussion of the measurements, results and a simulation. In the end conclusions will be drawn and there will be a look into the future of single molecule measurements.

## 2 Theory

### 2.1 A brief introduction to electrochemistry

Electrochemistry is a part of physical chemistry and it studies the electrical changes and chemical reactions at interfaces (e.g. between an electrolyte and an electrode). In these reactions charge is moved around between materials, e.g. between electrodes and molecules. The relevant part of electrochemistry for this report is the reduction-oxidation (redox) reaction.

The sensing mechanism of nanogap devices is based on redox cycling (figure 1). A redox reaction can be defined as the transfer of electrons between materials. A molecule gets oxidized by losing an electron by the process of oxidation, while gaining an electron makes the molecule reduced. Certain molecules can be oxidized and reduced repeatedly, making it able to be used in redox cycling. Molecules that can undergo redox reactions are able to transfer electrons from one electrode to the other in a solution. This transfer of electrons gives rise to a current. In redox cycling reversible redox-active molecules are reduced and oxidized repeatedly, greatly increasing the current. This process is shown in figure 1.

In the electrochemical measurements in this report two types of electrodes are used: Two working electrodes, the top and bottom electrode of the devices. These are the electrodes where the reactions take place that are researched; and a reference electrode in order to measure the potential differences.

The technique that is usually used to induce electrochemical processes is called cyclic voltammetry (CV). During CV measurements the potential of the working electrode is ramped to a certain potential and then it is ramped back to the starting potential.<sup>6</sup>

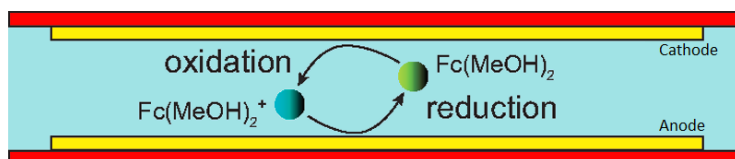


**Figure 1:** Redox cycling schematically. One molecule can undergo multiple redox reactions. Therefore the current is greatly increased.<sup>7</sup>

### 2.2 Why nanogap devices

Nanogap devices are formed by a narrow channel (height of  $z = 65$  nm in this case) and electrodes on both sides. These devices have certain advantages in detecting low concentrations of molecules. The current each molecule contributes is given by:<sup>4</sup>

$$i_0 = \frac{e \cdot n \cdot D}{z^2} \quad (1)$$

Here  $e$  is the charge of an electron,  $n$  is the number of electrons the molecule transfers and  $D$  is the diffusion coefficient. As can be seen in equation 1 the current is proportional to  $1/z^2$ . So in order to measure currents as accurately as possible and increase the signal to noise ratio, the electrodes have to be as closely spaced as possible. Furthermore a high aspect ratio (a long and narrow channel) gives rise to a high selectivity. So a high aspect ratio makes it easier to do research on specific molecules.<sup>8</sup>

### 2.3 Why is there a need for a new method?

The type of measurements currently used to detect single molecules are continuous current measurements. In these measurements an oxidizing and reducing potential is applied, as shown in Figure 2a, at which redox cycling can occur. Then the solution containing a certain amount of 1,1-ferrocenedimethanol (referred to as redox species from now on) in 0.1 M potassium chloride, which acts as a supporting electrolyte, is added. The next step is to wait and see if a signal due to a redox species is observed.

In figure 2 two graphs with results of such a measurement are shown. Each graph has two lines corresponding to the current measured at the bottom (black) and top (red) electrode. Figure 2b is a

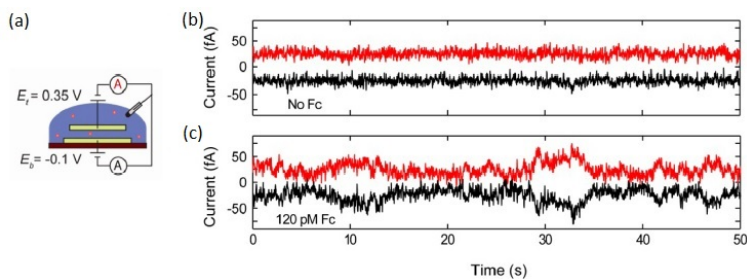


**Figure 2:** (a) Both electrodes are held at fixed potentials between which redox cycling is possible. (b) The upper graph shows the result for a continuous current measurements where there is no redox species in the solution. The lower graph shows the result for the same kind of measurements, but this time with 120 pM redox species ( $\text{Fc}(\text{MeOH})_2$  in this case). The anticorrelated signals are due to 0.4 redox species being present in the channel on average.<sup>4</sup>

continuous current measurement where there are no redox species in the nanochannel and the signal is just random noise. Figure 2c is a measurement where there is a small amount of redox species (120 pM) in the channel. The anticorrelated steps that can be observed means that a redox species has entered the channel and transferred electrons.<sup>4</sup> Every redox species contributes to the reactions multiple times making measuring individual redox species with the use of a nanochannel possible. The problem with this method is that it is very prone to noise. If the experimental setup is touched or moved, there will be a current due to noise that is much bigger than the tens of femtoampere that is observed from a single redox species interaction or if a big electromagnet in some other part of the building is switched on, the measurements are useless too. This makes it hard to integrate this method in devices.

A possible solution to circumvent this problem is to let one electrode float while applying a cyclic potential to the other. Due to redox cycling charge will build up on the floating electrode. By measuring this charge, the concentration of the solution could be characterized. This method should be less sensitive to noise. Exploring this idea is the goal of this report.

## 2.4 Expectations

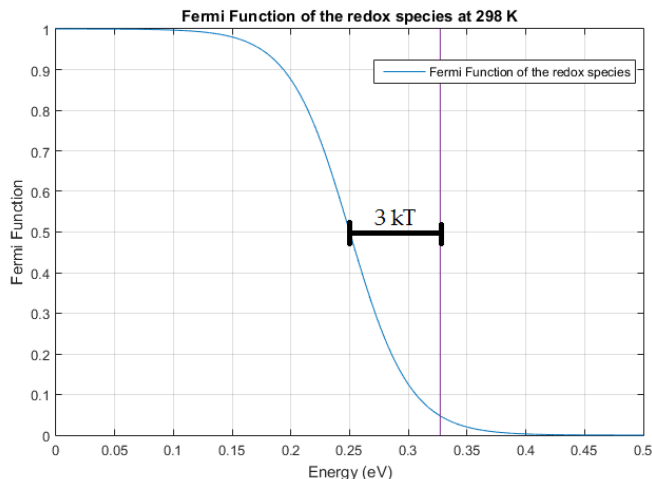


**Figure 3:** The Fermi-Dirac distribution for 1,1-ferrocenedimethanol at 298 K.

In the experiments one electrode is left floating, while a cyclic potential is applied to the other. Certain outcomes are expected. The potential of the floating electrode should follow the electrode on which a potential is applied. This is because the floating electrode wants to be in equilibrium with the nearby

solution and the solution wants to be in equilibrium with the cycled electrode. This can only be achieved by transferring charge between the two electrodes by the redox species. If the concentration of redox species is increased the potential of the floating electrode should follow the applied potential better (or faster). This is expected because if the concentration gets higher, there will be more redox species in the solution. If there are more redox species, more charge can get transferred, increasing the ability to influence the potential of the floating electrode. Thus at low concentrations the floating electrode follows the cycled electrode poorly, causing a low slope and peak-to-peak value. If the concentration is increased the slope will get steeper and the peak-to-peak value will get higher, as is illustrated in figure 4.

At higher concentrations a cutoff is expected, because for redox cycling to happen a certain electrode potential is needed. The standard potential for 1,1-ferrocenedimethanol reaction is 250 mV.<sup>7</sup> The rate of electron transfer is proportional to the Fermi-Dirac distribution, figure 3 and equation 2:

$$f(E) = \frac{1}{e^{(E-\mu)/kT} + 1} \quad (2)$$

Here  $E$  is the energy with respect to the solution potential (in eV),  $\mu$  is the standard potential (in eV),  $k$  is Boltzmann's constant and  $T$  is the absolute temperature. The chance for redox cycling to happen, is too small if the standard potential is exceeded by a few  $kT$  (where 'a few'  $\approx 3$ ). Therefore a cutoff is expected somewhere between 300 and 350 mV, as is shown in figure 4.<sup>9</sup> This idea was the starting points for the research presented here.

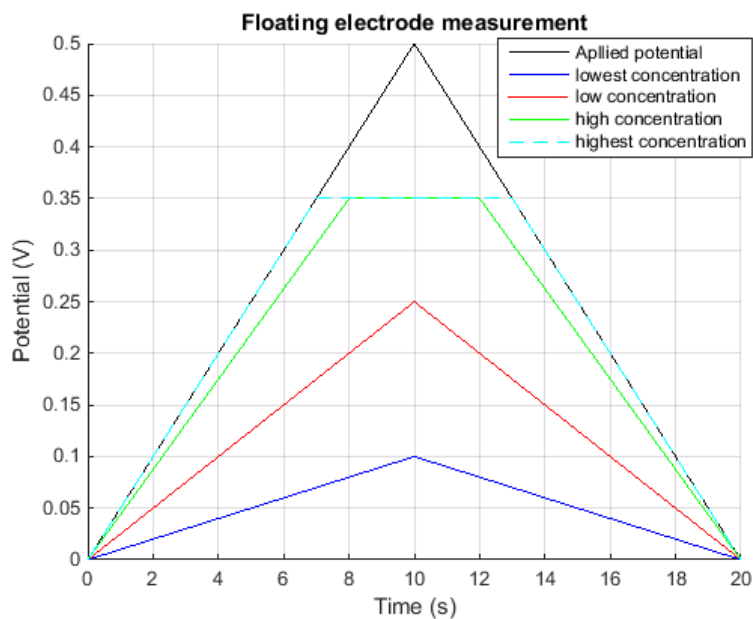


**Figure 4:** Qualitative expected results for a measurements were the concentration is varied. For higher concentration a higher peak-to-peak value is expected. The cutoff is predicted using the Fermi-Dirac distribution and will occur around 350 mV.

For the scan rate (the scan rate is defined as the step size per second of the applied potential) dependent measurements the peak-to-peak value should increase with decreasing scan rate, since the longer the electrode is charged the more charge the floating electrode will accumulate. In other words with lower scan rates it is easier for the floating electrode to keep up with the electrode that is being swept and to reach saturation.

### 3 Experimental Setup

#### 3.1 Device fabrication and geometry

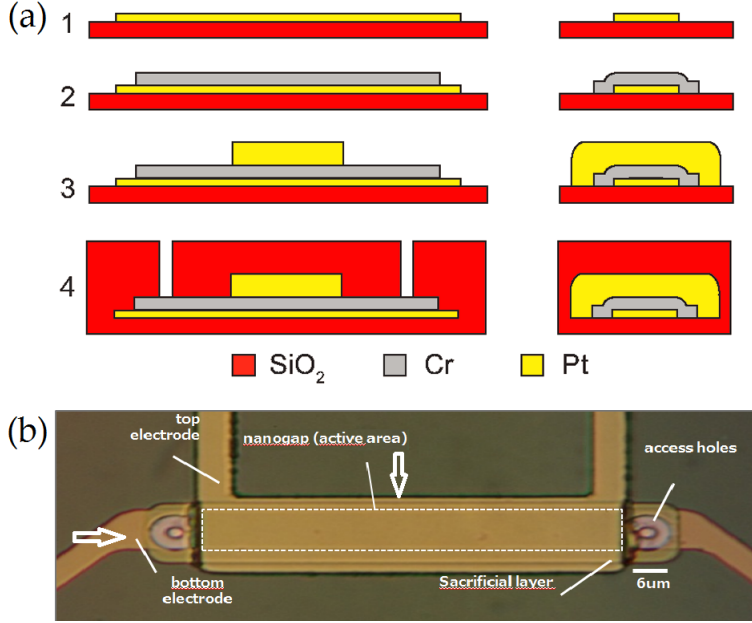


**Figure 5:** (a) Cross-sections of the device during fabrication. The cross-sections on the left correspond to the long axis, the vertical arrow in (b). The right cross-sections correspond to the short axis, horizontal arrow. 1 - A layer of silicon dioxide is thermally grown. A 15 nm high platinum electrode is deposited on top. 2 - A 65 nm high sacrificial chromium layer is evaporated on top of the platinum. 3 - A 60 nm high platinum electrode is deposited on top of the chromium. 4 - The device is passivated with a  $\sim 550$  nm layer of silicon dioxide. Access holes to the chromium layer are then etched. These schematic drawings are not to scale.<sup>7</sup> (b) a microscopic image of a finished device before etching (top view).

The fabrication of the nanofluidic channels used in the experiments, is shown schematically in figure 5a. All devices are fabricated on a standard silicon wafer. First a layer of silicon dioxide is thermally grown on the entire wafer. On top of the silicon dioxide layer the 20 nm high platinum bottom electrode is deposited using electron-beam evaporation, the width and length of the electrode depend on the device. Secondly, a layer of chromium is evaporated on top of the platinum layer. This chromium layer is 65 nm high and functions as a sacrificial layer. When the fabrication is finished, the chromium layer will be etched away, creating the nanochannel. The third step is the deposition of the 60 nm high platinum top electrode on top off the chromium. The fourth step is the passivisation of the device by evaporating a  $\sim 550$  nm silicon dioxide layer. Access holes to the chromium layer are then etched using ion etching.

In figure 5b a microscopic image is shown of a finished device before etching (top view).<sup>7</sup>

For the experiments devices with different shapes are used, see table 1. The difference between these devices lies in the sizes of the electrodes, the size of the holes and the distance between the holes and the top electrode. In figure 6 a schematic top down view is given of a device. BE and TE are the bottom and top electrode respectively. SR is the sacrificial layer. The sizes of BE, SR and TE, and the length of  $L_a$ ,  $L_e$  and  $L_d$  (see figure 6) are given in table 1. The number of access holes and the size of the access holes are given in the same table.

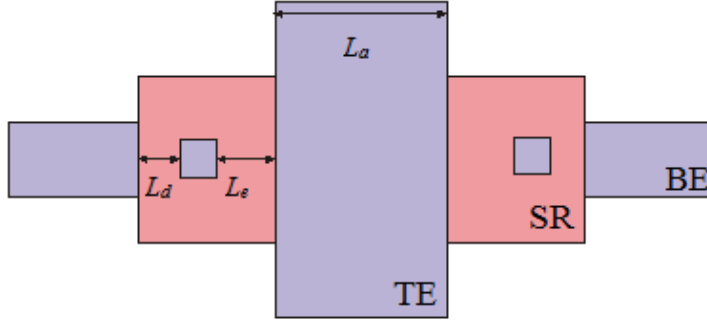


**Figure 6:** A schematic top down view of a device. BE and TE are the bottom and top electrode respectively. SR is the sacrificial layer. All the distances and sizes are given in table 1.

Device	$L_a$ ( $\mu\text{m}$ )	$L_e$ ( $\mu\text{m}$ )	$L_d$ ( $\mu\text{m}$ )	Width of BE ( $\mu\text{m}$ )	Width of SR ( $\mu\text{m}$ )	Width of TE ( $\mu\text{m}$ )	Size of access hole ( $\mu\text{m} \cdot \mu\text{m}$ )	Number of access holes
GD 2	10	2	2	3	5	7	$2 \cdot 2$	2
SMD 2	50	2	2	3	6	9	$2 \cdot 2$	2
SMD 3	50	2	2	3	5	7	$2 \cdot 2$	2
SMD 4	50	2	2	3	6	9	$2 \cdot 2$	1
SMD 5	50	2	2	3	5	7	$2 \cdot 2$	1

**Table 1:** Parameters for the used devices. BE and TE are the bottom and top electrode respectively. SR is the sacrificial layer. All other distances are defined in figure 6.

In figure 7 an optical image of a set of two devices is shown. On the left side of the image there are nine contact pads. The central contact pad is connected to a ultra micro electrode (UME). The top four are connected to a top device. The lower four to a lower device. Each electrode is connected to two contact pads in case one of them doesn't work and as a check to be able to measure the resistance of the wires and electrodes.

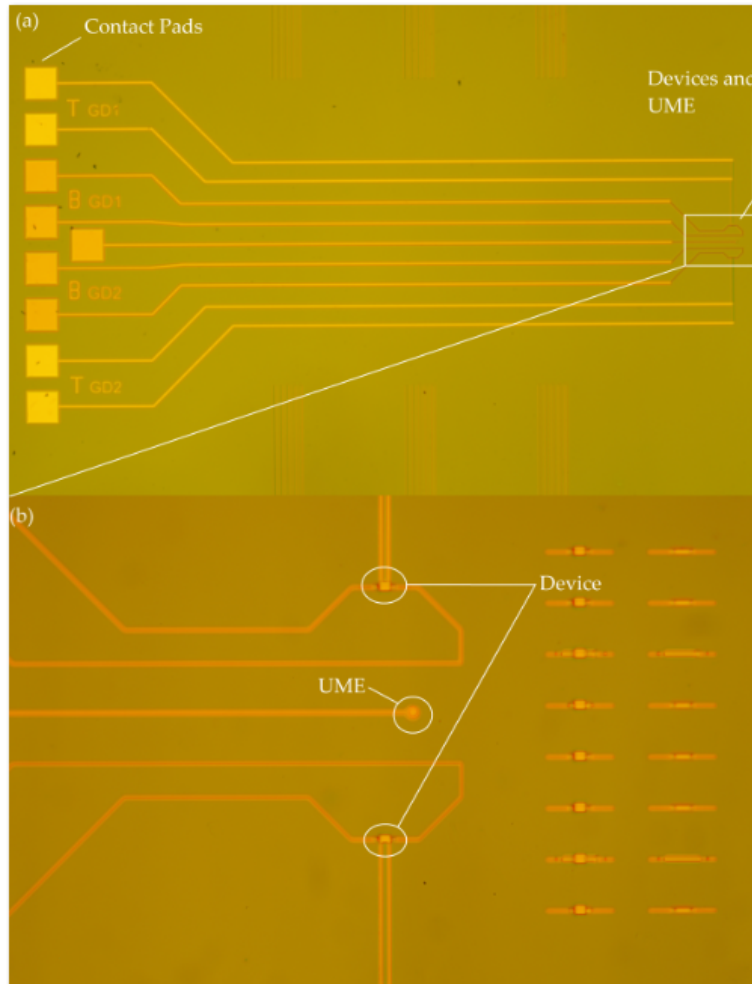


**Figure 7:** (a) Optical image of two devices. The electrodes are connected to contact pads via wires. (b) Zoom in of the two devices. Between the two devices the round UME is visible. On the right side of the figure test structures of each layer are present, in order to check if everything works properly.

### 3.2 Measurement preparation and setup

When using a new device for the measurements, the chip is thoroughly cleaned with acetone, isopropanol and purified water (milli-Q water). When reusing a device, it is only cleaned with milli-Q water.

A Polydimethylsiloxane (PDMS) plug is placed on top of one of the devices and acts as reservoir for the bulk solution. The top and bottom electrodes are connected as shown in figure 8. To start etching away the sacrificial layer a chromium etchant is put into the reservoir. By applying a small bias between the two electrodes a current starts flowing. When enough of the chromium is etched away, the electrodes no longer make contact and therefore the current drops to zero. To etch away the leftover chromium, the etchant is kept a little while longer in the reservoir. This is only done with a new device.

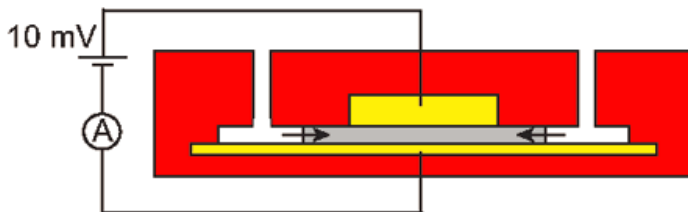


**Figure 8:** The current flow through the chromium layer is measured. When enough chromium is etched away, the electrodes no longer make contact and the current drops to 0.<sup>7</sup>

After etching or when reusing a device, the electrodes get cleaned with a 0.5 M sulfuric acid solution. The reservoir is filled with the sulfuric acid solution. An Ag/AgCl reference electrode (BASi, MF 2079, RE-5B) is placed in the bulk solution and on both electrodes a cyclic potential ranging from -0.15V to 1.2V is applied simultaneously. This is repeated for the top electrode while the bottom is floating and vice versa.

For the potential measurement the bottom, top and reference electrode are connected as shown in figure 9a. This setup keeps the bottom electrode floating, while a cyclic potential is applied to the top electrode. Different concentrations of redox species in 0.1 M potassium chloride, which acts as supporting electrolyte, are put into the PDMS plug. The top electrode is then scanned with different scan rates. The concentrations and scan rates used are given in the graphs in section 4 Results and Discussion.

When applying the cyclic potential to the bottom electrode, while the top is floating, everything is connected as in figure 9b.

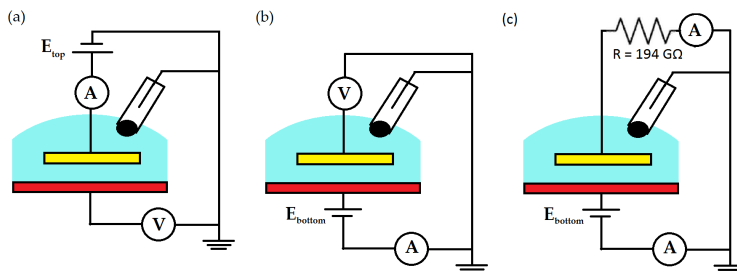


**Figure 9:** (a) A cyclic potential is applied to the top electrode (yellow) while the bottom electrode (red) is left floating. The current through the top electrode and the potential build up on the bottom electrode are measured. The reference electrode (white) is inserted in the bulk solution. (b) Now top is left floating, while a cyclic potential is applied to the bottom electrode. (c) Diagram for the measurements where the femto with a 194 GΩ is used.

For the initial measurements, the cyclic potential was applied and the cyclic voltammograms were measured using a variable gain sub femto ampere current amplifier DDPCA-300 (shortened to Femto). The Femto is connected to the computer via a National Instruments shielded I/O connector block (SCB-68). The potential on the bottom electrode is measured using a Keithley model 617 programmable electrometer (shortened to Keithley). Both the Keithley and the Femto are controlled with in-house Labview software.

For the later measurements, the Keithley is replaced by another Femto in series with a resistance of 194 G $\Omega$  (figure 9c). The potential can be determined by multiplying the measured current with the 194 G $\Omega$ .

## 4 Results and Discussion

### 4.1 Results

#### 4.1.1 Concentration dependent measurements

In figure 10a the results are shown for a measurement where the concentration is varied, the scan rate is 5 mV/s. The aim of this measurement is to see if the peak-to-peak values are concentration dependent. In this measurement the bottom electrode is left floating and the top electrode is swept (figure 9a) from 0 to 0.5 V and back, as the dash-dot line in figure 10a illustrates. For comparison of the peak-to-peak values, an offset correction has been done as seen in 10b.

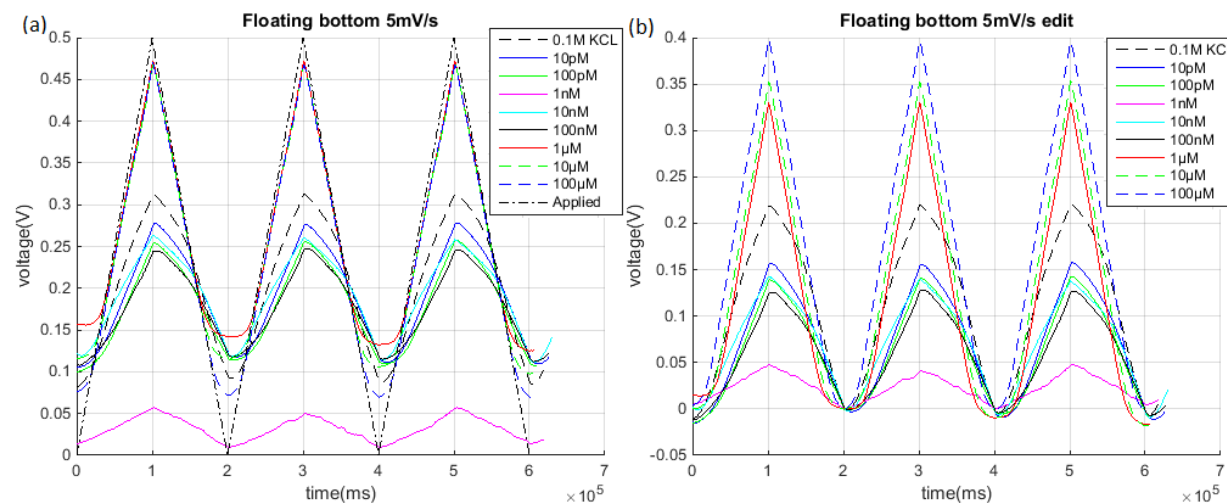


**Figure 10:** (a) Floating bottom measurements at 5 mV/s, the concentration is varied from no redox species to 100  $\mu\text{M}$  redox species in 0.1 M KCl. (b) Edited version of (a) in order to make it easier to compare the curves. Measured with SMD 2.

In figure 10a there are two regimes, the first regime consists of curves from 1  $\mu\text{M}$  to 100  $\mu\text{M}$ . Here, as expected there is a steady increase in potential of the floating electrode with increasing concentrations (as can be seen in figure 10b). The second regime is from 0.1 M KCl to 100 nM. In this regime the peak-to-peak values look randomly distributed and there is no increase in the peak-to-peak values with higher concentrations.

The randomness of the peak-to-peak values at lower concentrations could be due to an error in the solutions that are used, but this randomness is seen during different measurements, making this unlikely.

A more likely explanation could be that the measurement is very sensitive to contamination and that the cleaning process isn't thorough enough. Since a lot of experimental tools have to be cleaned for the experiments, things can get easily contaminated. This contamination could influence the results.

Another thing is that it could just be that it is not possible to measure very low concentrations with the method that is used. A reason for this can be that at low concentration some of the redox species are adsorbed, together with that the devices consist of 50 percent dead volume (volume in the device where there are no electrodes on both side).<sup>10</sup> This dead volume means that some redox species don't take part in the transfer of charge. This can be checked by doing the measurements at higher temperatures, higher temperature means less adsorption, and check if the peak-to-peak values does increase with increasing concentration.

Furthermore a thing that stands out is the 1 nM curve which is at a completely different equilibrium potential than the other curves. This is surprising. This could be due to air being trapped inside the reference electrode or solution, but this is checked after the measurements and this is not the case. The peak-to-peak value of the 1 nM is low in comparison to the other curves, this together with the offset probably means that something else is going wrong with this measurement. What exactly is going wrong

is unknown.

In figure 11a the result of a measurement where top is left floating and the bottom electrode is swept is shown (as shown in figure 9b). The scan rate is again 5 mV/s. Here the same issues are seen as are observed with the bottom electrode. In figure 11b the edited result is shown.

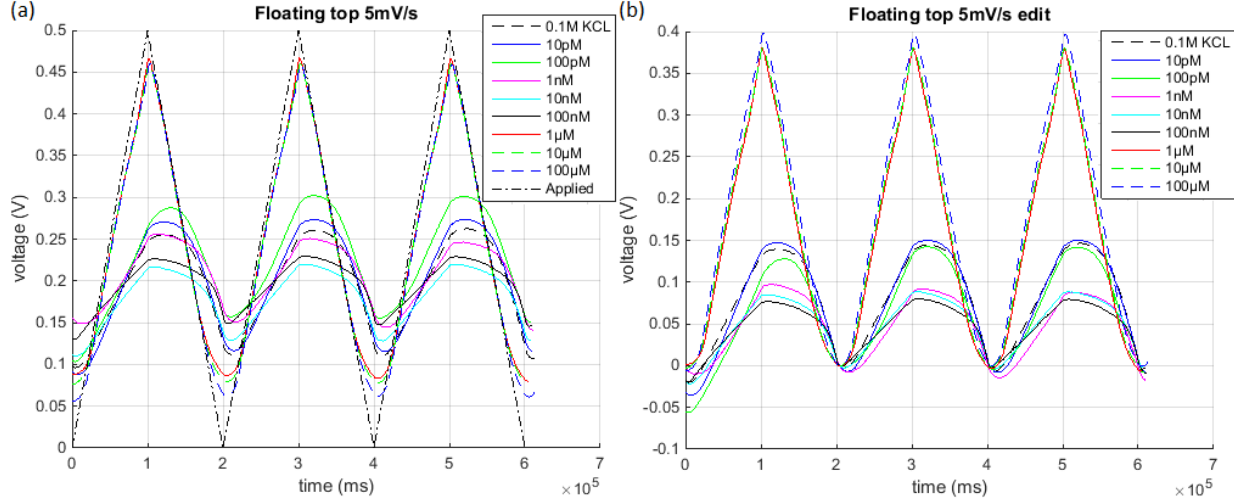


**Figure 11:** (a) Floating top measurements at 5 mV/s, the concentration is varied from no redox species to 100 uM redox species in 0.1 M KCl. (b) Edited version of (a) in order to make it easier to compare the curves. Measured with SMD 2.

In figure 11b it can be seen that the peak-to-peak value of the 100 μM curve is approximately 0.4 V and thus exceeding the value where a cut off was expected, namely 350 mV. The cutoff value was predicted using the Fermi-Dirac distribution, where it is assumed that the cutoff would occur a few  $kT$  above the standard potential of the redox species. According to the Fermi-Dirac distribution, the chance for redox cycling to happen is small. In practice a few redox species do undergo redox cycling beyond 350 mV and since the current is integrated over the time to get the charge that is transferred. The floating electrode can follow beyond 350 mV towards 400 mV.

#### 4.1.2 Concentration dependent simulation

To get a better understanding of the results, a simulation is performed. In this simulation the top electrode is swept and the bottom electrode is left floating. In order to achieve this the Butler-Volmer formalism is used:<sup>11</sup>

$$I_t^c = -I_b^c = i_{lim} \frac{\frac{1}{1+e^{-f\eta_t}} - \frac{1}{1+e^{-f\eta_b}}}{1 + \frac{D}{k_0 z} \left( \frac{e^{\alpha f\eta_t}}{1+e^{f\eta_t}} + \frac{e^{\alpha f\eta_b}}{1+e^{f\eta_b}} \right)} \quad (3)$$

Here  $f = F/RT$ ,  $F$  is the Faraday constant,  $R$  the gas constant and  $T$  is the absolute temperature.  $\eta$  is the overpotential applied to the top and bottom electrodes,  $\eta = E_{t,b} - E'_0$ . Here  $E_{t,b}$  is the potential at the top and bottom electrode, respectively and  $E'_0$  is the formal potential.  $k_0$  is the heterogeneous rate constant,  $\alpha$  is the transfer coefficient and  $i_{lim}$  is the limiting current, which is given by:<sup>7</sup>

$$i_{lim} = \frac{nFADc_B}{z} \quad (4)$$

Here  $A$  is the area of the electrodes and  $c_B$  is the concentration of the bulk solution. During the simulation  $E_t$  was given as input and  $E_b$  was 0.1 V initially (taken from the experimental results). These values are put into the Butler-Volmer formalism (equation 3) and together with the capacitance, the charge that is transferred was calculated. This charge is added to  $E_b$ , to get the new value of  $E_b$  (using equation 5). This process is repeated for every value of  $E_t$  and gives the self-consistent result that is shown in figure 12.

$$E_b(new) = E_b(old) + dt \frac{I_{rc}}{C} \quad (5)$$

Here  $dt$  is the time step between two values of  $E_t$  and  $C$  is the capacitance of the device.

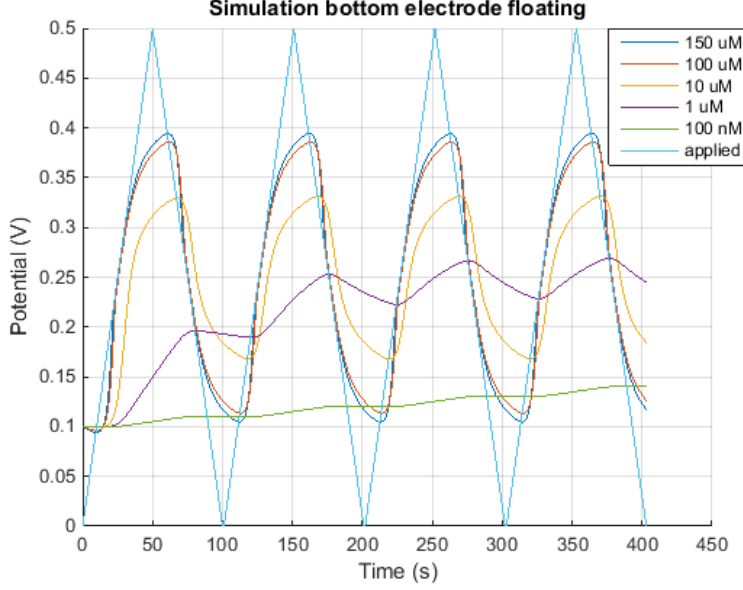


**Figure 12:** Simulation of the floating bottom electrode. All parameters used in this simulation are found in Shuo Kang's PhD thesis (2014).<sup>10</sup>

The signal for 100 nM is very low in the (idealized) simulation. Compared to the experiments, this suggests that what is measured at 100 nM and lower is a background effect and that the signal is too low to be measured with the used measuring equipment. Two things are very clear from the simulation: one is that the equilibrium position of the curves appears around 250 mV, which is  $E_0$ ; the other thing is that maxima and minima of the curves intersect with the applied potential. This makes sense since as long as the applied potential is larger than the floating potential, the floating potential increases (current flows from the cycled to the floating electrode). The floating potential decreases once the applied potential is smaller than the floating potential (current starts to flow from the floating to the cycled electrode). As the voltage/current relationship for a capacitor suggests:

$$dE = \frac{1}{C} I dt \quad (6)$$

Here  $dE$  is the potential change of the floating electrode and  $I$  is the current flowing through the cycled electrode.

When the simulation and measurement results are compared, it is clear that there is a difference in the peaks of the graphs. In the results the peaks are pointy and at the center of the CVs. Probably there is a parasitic effect dominating when the applied potential is around its peak. The dips of the curves look like the simulation; they shift a bit to the right when the peak-to-peak value gets lower. Furthermore the fact that our results show that 100 nM is the limit, with the measuring equipment that is used, is supported by the simulation.

### 4.1.3 Scan rate dependent measurements

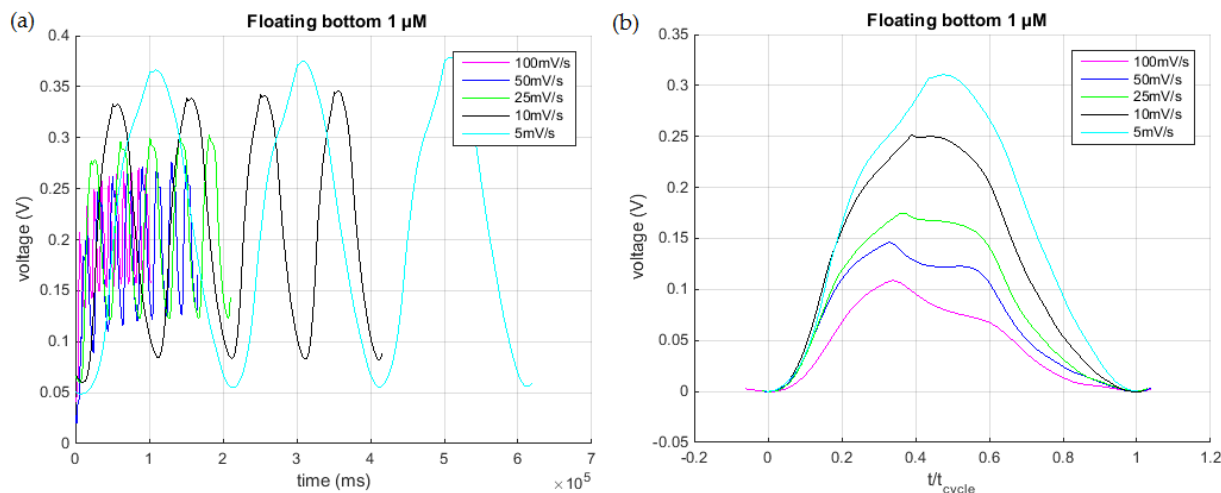


**Figure 13:** (a) Raw data of a measurements where the concentration was kept constant and the scan rate is varied. (b) Edited version of (a), one peak is chosen and cut out and normalized, to make it easier to compare the graphs. Measured with SMD 5.

In figure 13a the results are shown for a measurement where the concentration ( $1 \mu\text{M}$ ) is kept constant, but where the scan rate is changed. The graph in figure 13b is an edited version of the left one. For comparison one cycle is chosen and the curves have been normalized. As can be seen a higher scan rate means a lower peak-to-peak value, as was qualitatively expected.

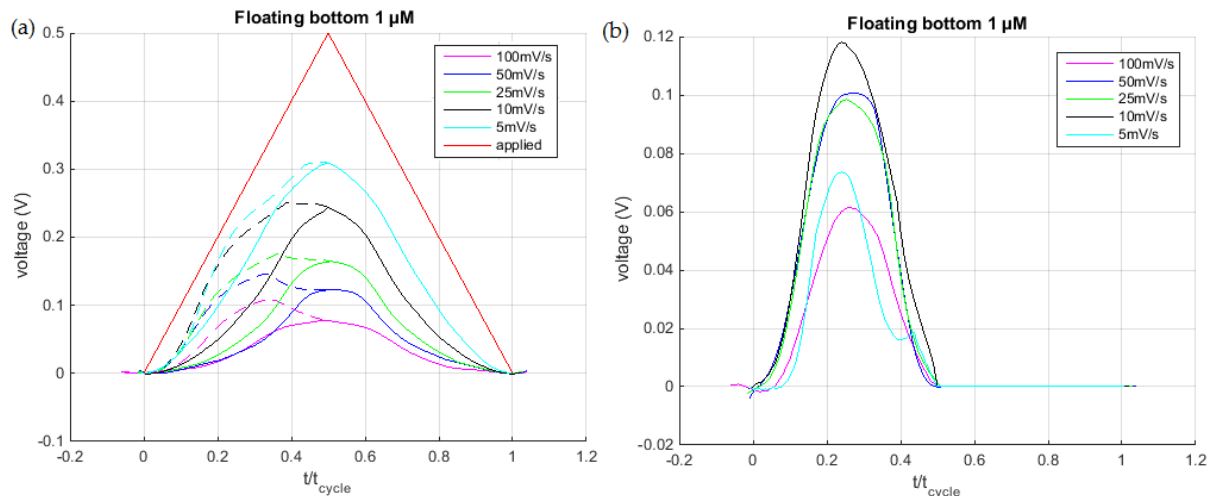


**Figure 14:** (a) Edited version of 13a where the right part (0.5 to 1 on the x axis) is mirrored to the left. The dashed line is the original curve and the solid line is the mirrored curve. (b) The curves are obtained by subtracting the solid line from the dashed line.

In the graph in figure 13b the first half of the scan (from 0 to 0.5 on the x-axis) the shape of the curves are a bit off (there is a extra peak), where the second half looks as expected. In order to investigate and quantify these anomalies, the second half of the graph is mirrored and the new curve is subtracted from the original one (as illustrated in figure 14a). The dashed line is the original curve.

Figure 14b shows the result if the graphs are subtracted from each other. The "errors" differ at most a factor two when the peak-to-peak values are compared. Since the scan rate is changed by a factor of 20

and the anomalies only change a factor of two, it could be that these anomalies are due to the same effect. The charge transferred is the current integrated over the time. A slower scan rate should therefore yield a higher transferred charge. The charge that this effect transfers is scan rate independent, which means that the effect is instant, e.g. a sudden desorption of redox species of the electrode. What effect this precisely is needs to be investigated in future experiments.

## 4.2 Possible problems with potential measurements in nanochannels

### 4.2.1 Instruments used in the measurements

One of the problems during the experiments is the measuring equipment. At first a high-end Keithley source meter (model 6430) is used to measure the potential at the floating electrode. The problem with the Keithley is that it shows drifts and offsets in the measurements, as can be seen in figure 15a. Especially at low concentration this drift is significant.

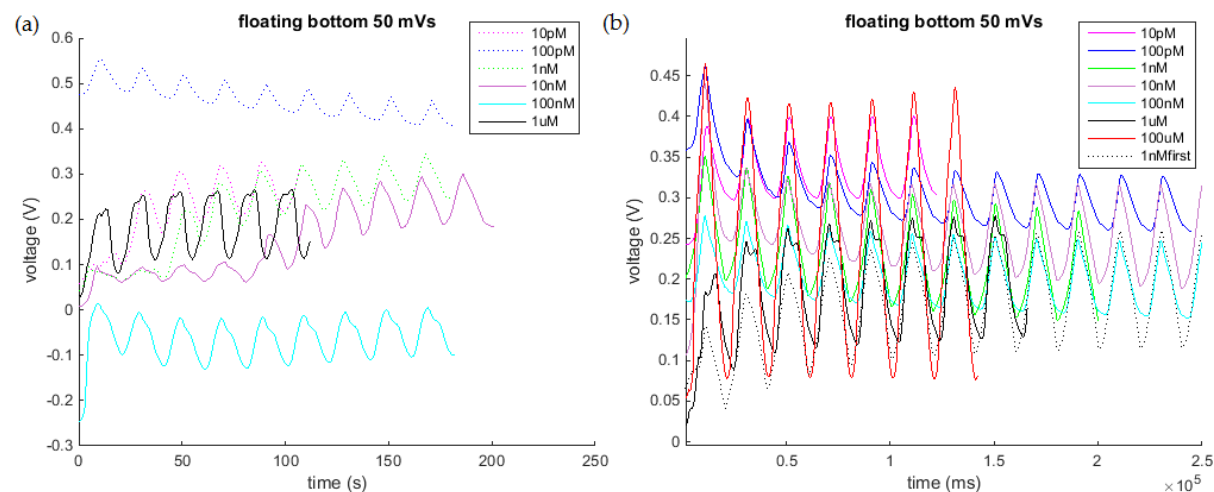


**Figure 15:** (a) Floating bottom electrode measurements, where the concentration is varied. Measured with the Keithley and SMD 2. (b) Floating bottom electrode measurements, where the concentration is varied. Measured with the femto and a  $194\text{G}\Omega$  resistance and SMD 5.

Due to the drift and offset differences the data becomes unreliable and harder to interpret. To overcome these problems a different way of measuring is used. The femto combined with a  $194\text{G}\Omega$  resistance is used to measure the floating electrode, as is illustrated in figure 9c. As can be seen in figure 15b the offset became a lot less, just several millivolts, which is probably due to the fact that different reference electrodes were used for every concentration and each reference electrode has its own, slightly varying, set potential.

But because the femto measures the current that passes through the  $194\text{G}\Omega$  resistance, it can't be said how much of the current has leaked away, because it has to pass a huge resistance. So there is no certainty that the signal is measured properly.

### 4.2.2 Reusability of the devices

Between two days of measuring, the devices have to be stored. This is done in either a  $0.5\text{mM}$  solution of sulfuric acid or milli-Q water. These storage methods alter the surface of the electrodes in the channel. Therefore the exact same measurement can yield two different results. This is shown in figure 16.

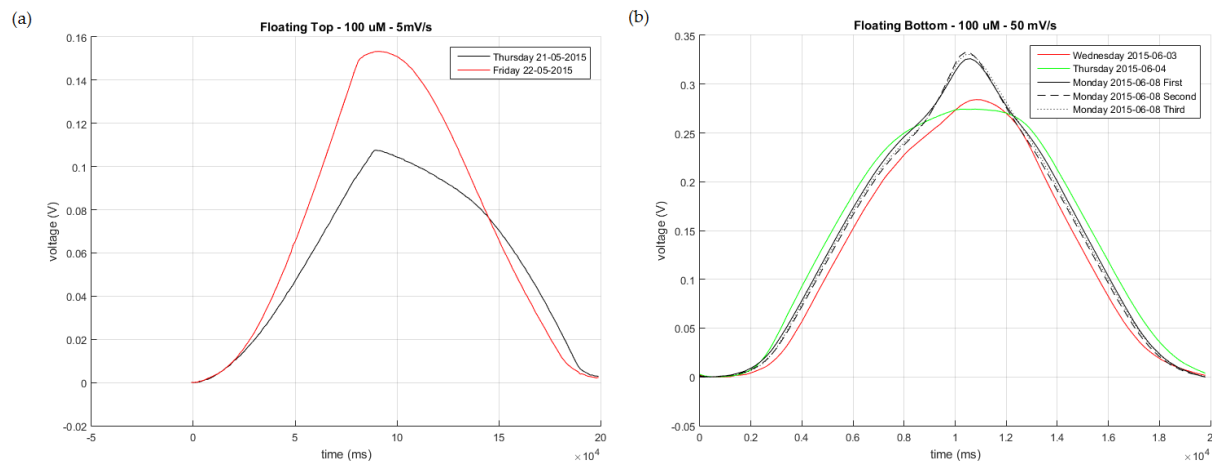


**Figure 16:** Different results for the same measurement done on two different days. Between the measurements in graph (a) the device (SMD 2) was stored in sulfuric acid. Between the measurements in graph (b) the device (GD 2) was stored in milli-Q water.

Figure 16a shows the voltage as function of the time. The bulk is a 1 nM redox species solution, and the potential over the top electrode is being measured. The scan rate of the top electrode is 5 mV/s. The graph shows two measurements done on two different days. Between these two days, the device is stored in a 0.5 mM sulfuric acid solution. The measurements are the same, but the results are different. The peak-to-peak value for the first day measurement is 0.1075 V, the peak-to-peak value for the second day measurement is 0.1532 V.

Figure 16b again shows the voltage as function of the time. This time the bulk is a 100 uM redox species solution. The potential over the bottom electrode is measured. The scan rate is 50 mV/s. The graph shows five measurements done on three different days. Between the three days, the device is stored in milli-Q water. Again the same measurement yields different results. The three measurements done on the same day differ a little bit. The solution between the first and second measurement is refreshed. This could explain the difference between the measurements on the same day. The peak-to-peak value is around 0.326 V. The peak-to-peak value for the first two days are 0.2841 V and 0.2735 V respectively. It is possible that the surface of the electrodes changes during storage. This is a problem when the device has to be used several days in a row.

### 4.3 Possible improvements for further research

Detecting lower concentration than achieved in this report should be possible with the use of electrochemistry. In order to achieve this some changes have to be made. The equipment that is used has to be more sensitive, since the simulation showed that the potential of the floating electrode at concentrations lower than 100 nM is tiny. Another thing is that the effect that causes the background reaction has to be removed or quantified, so that the signals at low concentration can be interpreted. Furthermore decreasing the amount of dead volume that is in the devices should help a lot. Since the used devices consist of 50 percent dead volume, roughly 50 percent of the molecules inside the channel don't participate in the transfer of charge.

## 5 Conclusion

In this report the influence of the concentration and scan rate on the ability of the floating electrode to follow the cycled electrode is researched and the following is concluded.

At higher concentrations (1  $\mu\text{M}$  and up) the floating electrode follows as expected. A higher concentration gives a better following. However at lower concentrations (below 100 nM) this doesn't work. The limit seems to lie between 100 nM and 1  $\mu\text{M}$ .

The scan rate dependency is as expected. The floating electrode follows better when the scan rate is slower.

Furthermore a simulation of the concentration dependency is performed to get a better understanding of the results.

To improve these experiments, several steps can be taken. To be able to measure the potential reliably, better measurement equipment is needed. To ensure that the results are reproducible, a better way to store the devices has to be found.

The same experiments, but at higher temperatures can be performed, in order to investigate if lowering the adsorption of redox species has an effect on the results. Looking what kind of effect dominates the measurements at lower concentrations is also a good subject for future experiments.

## 6 Appendix

### References

- [1] A. Armani, R. Kulkarni, S. Fraser, R. Flagan, and K. Vahala. Label-free, single-molecule detection with optical microcavities. *Science*, 317:783–786, 2007.
- [2] J.A. Bard, F.F. Fan, J. Kwak, and O. Lev. Scanning electrochemical microscopy. introduction and principles. *Anal. Chem.*, 61:132–138, 1989.
- [3] J. Kwak and J. Bard. Scanning electrochemical microscopy. theory of the feedback mode. *Anal. Chem.*, 61:1221–1227, 1989.
- [4] S.G. Lemay, S. Kang, K. Mathwig, and P.S. Singh. Single-molecule electrochemistry: Present status and outlook. *Acc. Chem. Res.*, 46:369–377, 2012.
- [5] M.J.J. Van Megen, M. Odijk, J. Wiedemair, W. Olthuis, and A. Van den Berg. Differential cyclic voltammetry for selective and amplified detection. *J. Electroanal. Chem.*, 681:6–10, 2012.
- [6] Allen Bard and Larry Faulkner. *Electrochemical Methods: Fundamentals and Applications*. Wiley, 2001.
- [7] M.A.G. Zevenbergen, B.L. Wolfrum, E.D. Goluch, P.S. Singh, and S.G. Lemay. Fast electron-transfer kinetics probed in nanofluidic channels. *J. Am. Chem. Soc.*, 131:11471–11477, 2009.
- [8] I. Vlasiouk, S. Smirnov, and Z. Siwy. Ionic selectivity of single nanochannels. *Nano Lett.*, 8:1978–1985, 2008.
- [9] Ralph Baierlein. *Thermal Physics*. Press Syndicate of the University of Cambridge, 2003.
- [10] Shuo Kang. *Single-Molecule Detection in Electrochemical Nanogap Devices*. PhD thesis, University of Twente, 2014.
- [11] S. Sarkar, K. Mathwig, S. Kang, A.F. Nieuwenhuis, and S.G. Lemay. Redox cycling without reference electrodes. *Analyst*, 139:6052–6057, 2014.